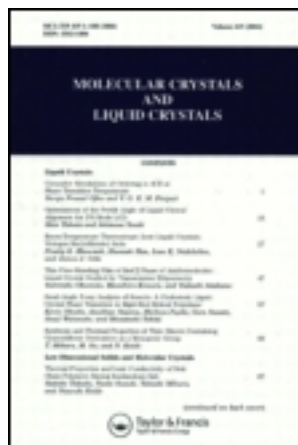


This article was downloaded by: [Tomsk State University of Control Systems and Radio]

On: 19 February 2013, At: 12:52

Publisher: Taylor & Francis

Informa Ltd Registered in England and Wales Registered Number: 1072954  
Registered office: Mortimer House, 37-41 Mortimer Street, London W1T 3JH, UK



## Molecular Crystals and Liquid Crystals Incorporating Nonlinear Optics

Publication details, including instructions for authors and subscription information:

<http://www.tandfonline.com/loi/gmcl17>

### Phonon Dispersion in a Deuterated 2,3-Dimethylnaphthalene Crystal at 123 K

F. Wörlen<sup>a</sup>, J. Kalus<sup>a</sup>, U. Schmelzer<sup>a</sup> & G. Eckold<sup>b</sup>

<sup>a</sup> Experimentalphysik I der Universität Bayreuth, Postfach 101251, D-8580, Bayreuth, BRD

<sup>b</sup> Institut für Kristallographie der RWTH Aachen, Templer-graben 55, D-5100, Aachen, BRD

Version of record first published: 19 Dec 2006.

To cite this article: F. Wörlen, J. Kalus, U. Schmelzer & G. Eckold (1988): Phonon Dispersion in a Deuterated 2,3-Dimethylnaphthalene Crystal at 123 K, Molecular Crystals and Liquid Crystals Incorporating Nonlinear Optics, 159:1, 297-314

To link to this article: <http://dx.doi.org/10.1080/00268948808075280>

PLEASE SCROLL DOWN FOR ARTICLE

Full terms and conditions of use: <http://www.tandfonline.com/page/terms-and-conditions>

This article may be used for research, teaching, and private study purposes. Any substantial or systematic reproduction, redistribution, reselling, loan, sub-licensing, systematic supply, or distribution in any form to anyone is expressly forbidden.

The publisher does not give any warranty express or implied or make any representation that the contents will be complete or accurate or up to date. The accuracy of any instructions, formulae, and drug doses should be independently verified with primary sources. The publisher shall not be liable for any loss, actions, claims, proceedings, demand, or costs or damages whatsoever or howsoever caused arising directly or indirectly in connection with or arising out of the use of this material.

# Phonon Dispersion in a Deuterated 2,3-Dimethylnaphthalene Crystal at 123 K

F. WÖRLEN, J. KALUS, and U. SCHMELZER

*Experimentalphysik I der Universität Bayreuth, Postfach 101251, D-8580 Bayreuth, BRD*

and

G. ECKOLD

*Institut für Kristallographie der RWTH Aachen, Templer-graben 55, D-5100 Aachen, BRD*

(Received October 27, 1987)

Coherent inelastic neutron scattering has been used to obtain phonon dispersion curves of fully deuterated 2,3-dimethylnaphthalene  $C_{10}D_6(CD_3)_2$ , which crystallizes in a lattice similar to naphthalene, but with dipolar structural disorder of the acentric molecules. The phonons have been observed at a temperature of 123 K for a wavevector  $\mathbf{q}$  along the  $[1,0,0]$ -direction. The agreement with data obtained from an earlier Raman experiment is good. Calculations of the lattice dynamics have been performed with the molecules taken as rigid bodies. Together with the results from Raman experiments the zone-center phonons were assigned to different types of molecular motions. The phonon linewidths are broad, which is attributed to dipolar disorder.

Mit kohärenter inelastischer Neutronenstreuung wurden Dispersionskurven für voll deuteriertes 2,3-Dimethylnaphthalin  $C_{10}D_6(CD_3)_2$  ermittelt, welches in einem ähnlichen Gitter wie Naphthalin kristallisiert, jedoch mit dipolarer struktureller Unordnung der azentrischen Moleküle. Es wurden Phononen bei einer Temperatur von 123 K für Wellenvektoren  $\mathbf{q}$  parallel zur  $[1,0,0]$ -Richtung untersucht. Die Übereinstimmung mit Daten einer früheren Ramanmessung ist gut. Berechnungen der Gitterdynamik wurden durchgeführt, wobei die Moleküle als starr angenommen wurden. Unter Einbeziehung der Ergebnisse aus Ramanexperimenten ließen sich die Phononen im Zonenzentrum den verschiedenen Typen der Molekülbewegung zuordnen. Aufgrund der dipolaren Unordnung sind die Phononenlinien stark verbreitert.

## 1. INTRODUCTION

At room temperature the acentric molecules of 2,3-dimethylnaphthalene  $C_{10}D_6(CD_3)_2$  “2,3-DMN” crystallize in a similar lattice as the

centrosymmetric naphthalene. The structure of naphthalene is monoclinic, space group  $P2_1/a$ , with two molecules in the unit cell; the same was found experimentally for 2,3-DMN. This implies that the molecules must be situated at centers of inversion. But since they do not possess a center of inversion, dipolar disorder had to be assumed, which was confirmed by x-ray crystal structural analysis.<sup>1</sup> The direction of the individual molecules, indicated by the arrows Z1 and Z2 for molecules "A" and "B" (see Figure 1b and 1c), are oriented in a random or nearly random way "up" and "down." The unit cell parameters of protonated 2,3-DMN at 300 K are:  $a = 0.7916(10)$  nm,  $b = 0.6052(8)$  nm,  $c = 1.0017(8)$  nm,  $\beta = 105.43(10)^\circ$ .<sup>1</sup>

Two phase transitions have been observed, one of higher order

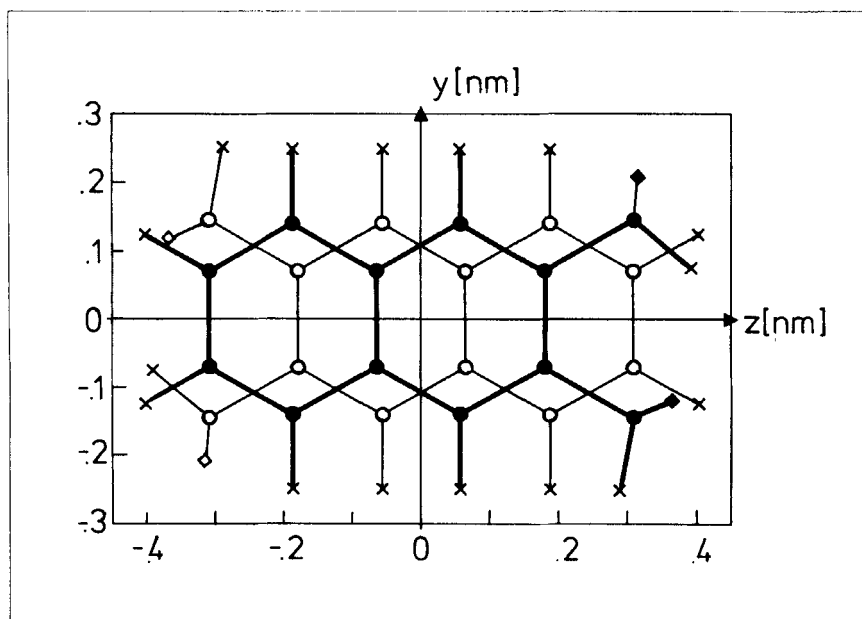


FIGURE 1 a) The constructed averaged molecule made by superposition of two 2,3-DMN molecules with opposite dipolar orientation. All atoms, except the H-atoms of the  $\text{CH}_3$ -group are in the plane of the molecule (see model 1). This average molecule is compatible with the x-ray diffraction data.<sup>1</sup> b) The unit cell of 2,3-DMN of model 2 (see text). The twofold molecular symmetry axis, indicated by an arrow, is always oriented up. The molecule B is related to A by the symmetry operation (glide reflection at the  $a$ - $c$ -plane) of the space group  $P_a$ . Units are in nm. c) The unit cell of 2,3-DMN of model 3 (see text). The twofold molecular symmetry-axis is indicated by an arrow. Molecule A is related to B by the symmetry-operation (screw diade operation) of the space group  $P2_1$ . In the real crystal these axis is statistically oriented up and down. Units are in nm.

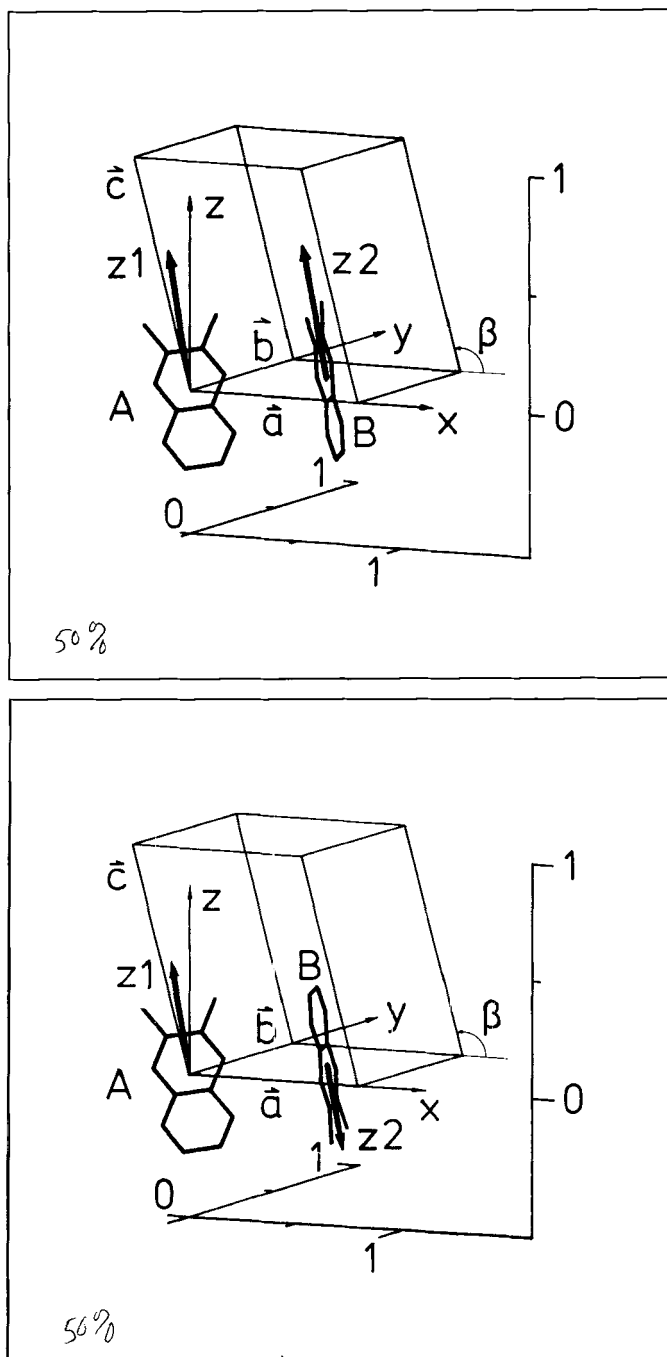


FIGURE 1 (continued).

from monoclinic to triclinic, occurring at 210 K, and another one at 110 K. Details of the low temperature structure are unknown.<sup>1</sup>

The quality of 2,3-DMN single crystals can be extremely good. Mosaic angles in the region of  $\leq 0.1^\circ$  even for bigger crystals can be obtained. Large regions of the crystals can be free of dislocations.<sup>2</sup> The crystals exhibit perfect cleavage parallel to the  $a$ - $b$ -plane.

Incoherent inelastic neutron scattering spectra of 2,3-DMN with different degrees of deuteration<sup>3</sup> yielded information about the phonon density of states  $g(\omega)$ . At 90 K a librational mode of the  $\text{CH}_3$ -groups was identified at an energy of 6.30 THz. The energy decreased to 4.34 THz for deuterated methyl groups. A decrease of this amount is expected due to the change of the moment of inertia, provided the libration takes place around the symmetry axis. Both incoherent inelastic neutron and Raman scattering experiments give evidence that the phonon spectra do not change substantially between 12 and 297 K.<sup>3</sup>

An estimate of the dynamics of the methyl groups was obtained with a so-called “fixed window” scan,<sup>4</sup> which measures the elastic or quasi-elastic intensity within the energy resolution  $\Delta E = 0.6 \mu\text{eV}$  of the spectrometer (“energy window”) as a function of temperature  $T$ .

A model taking into account a jump reorientational diffusion about the three-fold axis of symmetry was used to fit the experimental data. It turned out that a broad band of activation energies around a mean value of 1350 K had to be assumed. This was attributed to the dipolar disorder of the molecules mentioned above.

The aim of the present study was to obtain more information about the lattice dynamics of a disordered molecular crystal. We used coherent inelastic neutron scattering for determining phonon dispersion curves. Because of the loss of the strict translational invariance in the disordered crystal one has to expect broad phonon lines, even at very low temperatures.<sup>5</sup> This was found, indeed, by Raman measurements down to 12 K.<sup>3</sup>

The paper is organized as follows: in section 2 we discuss the sample preparation, the experimental set-up and results. An overview about calculations and models follows. Calculated dispersion curves are presented and the measured branches are assigned to the predominant character of the respective motion of the two molecules in the unit cell, i.e. the translations into the direction of the different axes of the crystal frame, or librations about these axes. Calculations and experimental results of a Raman measurement were helpful for obtaining and interpreting experimental dispersion curves, which follow from the present coherent inelastic neutron scattering experiments.

## 2. EXPERIMENTAL SET UP AND RESULTS

### 2.1. Sample preparation

Dimethylnaphthalene-2,3-dicarboxylate (Aldrich) was reduced with  $\text{LiAlD}_4$ /ether to the diol, which was then treated with 40% HBr-acetic acid to yield  $\text{C}_{10}\text{H}_6(\text{CD}_2\text{Br})_2$ . Reduction with  $\text{LiAlD}_4$  in tetrahydrofuran at  $65^\circ\text{C}$  gave  $\text{C}_{10}\text{H}_6(\text{CD}_3)_2$ ; that was converted to  $\text{C}_{10}\text{D}_6(\text{CD}_3)_2$  by exchanging the aromatic hydrogens. For this purpose it was treated with 65%  $\text{D}_2\text{SO}_4/\text{D}_2\text{O}$  (1.8 ml per mmol) at 413 K in a sealed ampoule for eight days. The reaction mixture was dissolved in ether, the ether solution extracted with base, concentrated and the residue sublimed *in vacuo*. The degree of deuteration of  $\text{C}_{10}\text{D}_6(\text{CD}_3)_2$  “2,3-DMN- $\text{d}_{12}$ ” was more than 97.5% as determined by  $^1\text{H}$ -NMR spectroscopy.<sup>3</sup>

The substance was zone refined several times. A single crystal with a mass of approximately 0.8 g was grown by the Bridgman method with a mosaic width of less than  $0.1^\circ$ . The crystal had the shape of half a cylinder with a cut along the cylinder axis. The “cut” was the cleavage plane ( $a$ - $b$ -plane). Cylinder axis and  $b$  axis include an angle of about  $60^\circ$ .

### 2.2. Neutron measurements

The measurements were performed on the triple-axis-spectrometer UNIDAS at the Kernforschungsanlage Jülich. The neutron incident energy was selected by the (0,0,2)-planes of a pyrolytic graphite double monochromator PG(002) with a vertical radius of curvature of 1.33 m and a mosaic spread of  $40'$ .

The analyzer PG(002) had a vertical radius of curvature of 0.72 m and a mosaic spread of  $40'$ . Incident and scattered neutron divergences between monochromator 1, monochromator 2, sample, analyzer and counter were defined by soller collimators of divergency  $1.10^\circ$ ,  $0.75^\circ$ ,  $0.75^\circ$  and  $0.75^\circ$ . For acoustic phonons near the  $\Gamma$ -point the collimation was reduced to  $0.40^\circ$ ,  $0.25^\circ$ ,  $0.25^\circ$  and  $0.25^\circ$  respectively. The spectrometer was used in the W-configuration. The measurements were performed with  $k_F$  fixed at  $26.62 \text{ nm}^{-1}$ . A pyrolytic graphite filter in front of the analyzer was used to avoid higher order contamination. Most of the phonons were measured for a constant momentum transfer  $\hbar\mathbf{Q}$  of the neutrons. Some acoustic phonons near the  $\Gamma$ -point however, were determined by keeping the energy-transfer of the spectrometer constant. In most cases the resolution of the

spectrometer was around 0.3 THz. The  $a^*-c^*$ -plane was chosen as scattering plane.

To avoid damage to the crystal during cooling, the temperature was changed with a cooling rate of 6 K/h (290–200 K) and 10 K/h (200–123 K), respectively. At the final temperature of 123 K, the measured lattice parameters for the deuterated substance were  $a = 0.769(1)$  nm,  $b = 0.593(1)$  nm,  $c = 0.989(2)$  nm and monoclinic angle  $\beta = 104.47(3)^\circ$ .

With the help of calculated dynamical structure-factors and from our experience with naphthalene we found Brillouin-zones with strong phonon intensities in the zone-center. In these zones we measured the phonons with wavevector  $\mathbf{q}$  parallel to the  $[1,0,0]$ -direction. In addition, some acoustic modes with  $\mathbf{q}$  parallel to  $[0,0,1]$ -direction were determined.

As an example the longitudinal polarized acoustic mode can be found in the  $[2,0,0]$ -zone. The transversal acoustic phonons polarized in  $c$ -direction could be detected with high intensity especially in the  $[0,0,3]$ -zone.

The frequencies of the phonons were obtained by intensity weighted least-squares fits to the given experimental data. Figure 2 shows a typical example for a scan. One can see the elastic line and a fit of three phonons upon a nearly constant background, which comes from incoherent and multiphonon scattering. The line shape of the phonons were assumed to be Gaussian. The halfwidths of the Gaussian curves fitted to elastic line and phonons are in the order of 0.30 THz and 0.38–1.00 THz, respectively. In most cases all parameters were varied freely. The large width of the phonon lines complicates the decomposition of the different phonons. The obtained phonon frequencies are given in Table I and the phonons are represented in Figure 3.

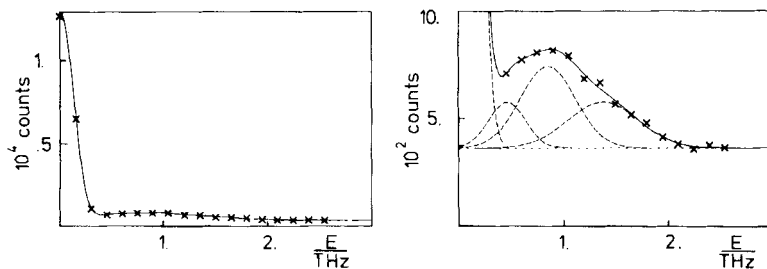


FIGURE 2 Example for a scan with  $\mathbf{Q} = (3.5, 0, -4)$ . The elastic line is caused by the disorder of the crystal. The inelastic region is shown in enlarged scale in the right-hand part of the figure. Three phonons were fitted to the experimental data.



TABLE I

The phonon frequencies (in THz) determined in the neutron scattering experiment. They are represented as dots in Figure 3.

$q/a^*$	Branch number as in Figure 3					
	1	2	3	4	5	6
0.0	—	—	0.54(2)	1.01(2)	1.44(6)	3.07(7)
0.1	—	0.39(1)	—	—	—	3.25(3)
0.2	0.28(2)	—	0.81(2)	—	1.34(2)	3.25(4)
0.3	0.45(2)	—	0.90(5)	1.27(3)	1.40(18)	3.25(9)
0.4	0.54(6)	—	1.06(3)	1.43(8)	1.69(4)	3.28(5)
0.5	0.54(8)	—	0.97(2)	1.37(2)	1.90(5)	3.52(9)
0.6	0.50(2)	0.71(2)	1.01(2)	1.39(9)	—	3.60(6)
0.7	—	0.65(4)	1.06(5)	—	2.46(12)	3.79(5)
0.8	—	0.65(4)	1.16(3)	1.54(3)	2.90(18)	3.82(12)
0.9	—	0.60(6)	1.15(5)	1.63(10)	2.96(11)	3.56(8)
1.0	—	0.55(3)	0.99(5)	1.43(10)	3.14(15)	3.68(18)

Since in x-ray measurements the crystal obviously shows symmetry with respect to inversion, we present the dispersion curves in the so-called extended zone scheme (see next section).

When inversion symmetry holds for 2,3-DMN, all librational modes are symmetric with respect to the inversion center, a symmetry-operation contained in the space-group of naphthalene, and are Raman active. The Raman spectra of 2,3-DMN did not change their feature on crossing the phase transition at 210 K and it can be assumed that this symmetry still holds approximately at 123 K. The results of Raman measurements<sup>3</sup> can be used to identify the librational modes at the  $\Gamma$ -point. In Table II measured neutron frequencies are compared with Raman results, displayed on the right side of Figure 3. The agreement is good.

### 3. MODEL CALCULATIONS

At the moment we are not able to calculate harmonic lattice dynamics of dipolarly disordered crystal rigorously. To get some idea about the influence of disorder we calculated the phonon frequencies for three model crystals, exhibiting perfect translational invariance. In the first model we constructed an averaged molecule in a crystal similar to naphthalene. In the other models we assumed the molecules in a crystal with lower symmetry.

The phonon frequencies were calculated using a model developed by Pawley.<sup>6</sup> This model assumes that molecules behave like rigid units. The interactions between two molecules are expressed as a

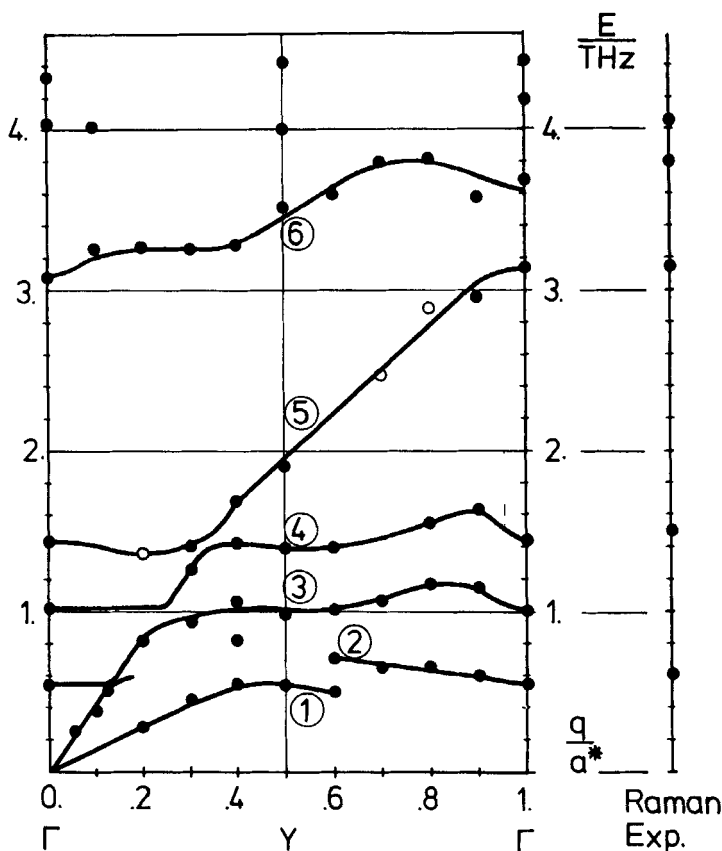


FIGURE 3 Measured dispersion curves for 2,3-DMN in an extended zone scheme for the wavevector  $\mathbf{q}$  parallel to the  $[1,0,0]$ -direction at a temperature of 123 K (see Table I). Open circles indicate weak intensities. For  $0 \leq q/a^* < 0.5$  the modes which are symmetric with respect to the reflection at the  $a^*-c^*$ -plane, and for  $0.5 < q/a^* \leq 1.0$  the antisymmetric ones are shown. The solid curves are guides to the eye. Results from Raman measurements (temperature 120 K; see Table II) are displayed on the energy-axis on the right-hand side for comparison.

superposition of atom-atom interactions between different molecules. The interaction potential is assumed to be of Buckingham type:

$$U_n(r_{ij}) = -A_n r_{ij}^{-6} + B_n \exp(-\alpha_n r_{ij}), \quad (1)$$

where  $r_{ij}$  is the distance between two atoms  $i$  and  $j$  of different molecules. The potential parameters  $A_n$ ,  $B_n$  and  $\alpha_n$  depend only on the different pairings of the atoms. The parameter set IV given by Williams<sup>7</sup> was used, assuming that C-D and D-D pairings are equivalent to

TABLE II

Frequencies (in THz) observed in Raman spectra of deuterated 2,3-DMN at different temperatures up to 7 THz (columns 1 to 5; from Reference 3), and frequencies observed at the  $\Gamma$ -point in the present neutron scattering measurement at 123 K (see column 6). In the last column the predominant character of motion (L for libration, T for translation) is indicated for these modes.

300 K	120 K	80 K	30 K	12 K	123 K	Character of the molecular motion
0.69	0.60				0.54(2)	L
					0.55(3)	L
					0.99(5)	T
					1.01(2)	T
1.35 <sup>a</sup>	1.50 <sup>a</sup>	1.35	1.47	1.59	1.43(19)	L
					1.44(6)	L
2.67	3.15	3.18	3.18	3.18	3.07(7)	L
					3.14(15)	T
		3.39	3.42	3.42		
3.66	3.81	3.84			3.68(18)	L
4.05	4.05	4.02	4.02	4.02	4.02	internal mode (?)
		7.11	7.11	7.08		

<sup>a</sup>Shoulder

C–H and H–H (see Table III). This parameter set reproduced structural data and phonon dispersion curves of several molecular crystals rather well, especially those of naphthalene and anthracene.

### 3.1. Model 1

According to the results of the x-ray structure analysis of Karl *et al.*<sup>1</sup> an averaged molecule, which was obtained by a superposition of two 2,3-DMN molecules was constructed (see Figure 1a). This averaged molecule shows inversion-symmetry and is, apart from the methyl groups, planar. The calculations were performed for a monoclinic crystal of space group  $P2_1/a$  like naphthalene with two molecules in the unit cell.

For the actual lattice-dynamical calculations we divided the values of the potential parameters  $A_n$  and  $B_n$  by 4, in order to take into account the doubled number of pseudo-atoms sitting in the averaged molecules.  $\alpha_n$  was not altered, because the shape of the potential (see Equation (1)) must be the same. The mass of the pseudo-atoms were divided by 2. In turn the unit cell parameters  $a$ ,  $b$ ,  $c$  and  $\beta$ , as well as the orientations of the molecules in the unit-cell were varied until

the minimum of lattice energy was reached. This procedure has been described in more detail in Reference 6.

As it is known<sup>8</sup> for a crystal of space group  $P2_1/a$  the little group  $G(\mathbf{q})$  for the  $[\xi, 0, \eta]$  direction contains a glide plane and the one for the  $[0, \xi, 0]$  direction a two-fold screw axis. Therefore we have in  $[\xi, 0, \eta]$  direction symmetric as well as antisymmetric modes with respect to the reflection by the  $a^*-c^*$ -plane. In Figure 4 (and also in Figure 3 and 5) the symmetric and antisymmetric modes are presented separately in so-called extended zone schemes. For a crystal with two

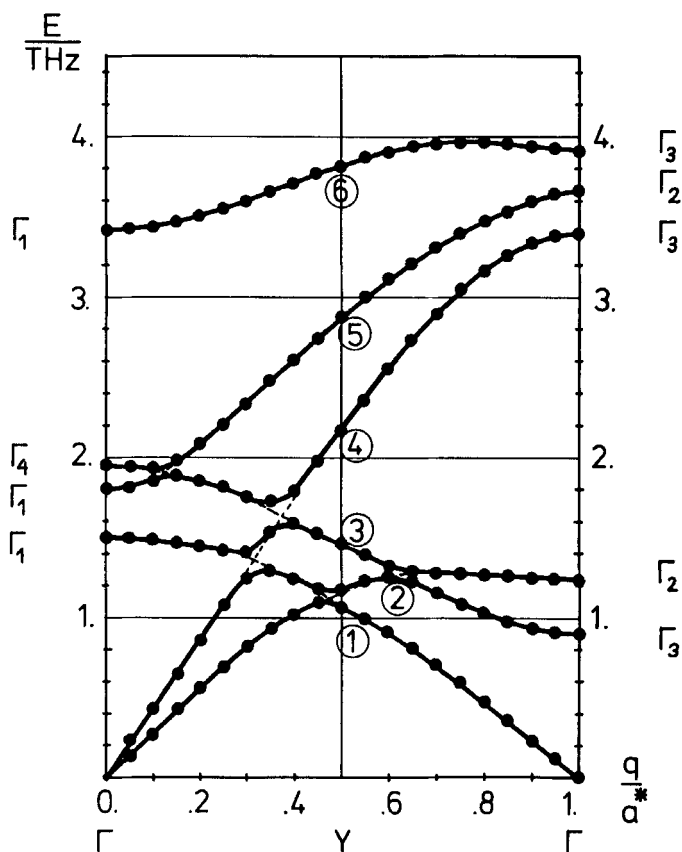


FIGURE 4 Calculated dispersion curves for 2,3-DMN in an extended zone scheme for the wavevector  $\mathbf{q}$  parallel to the  $[1, 0, 0]$ -direction using model 1 (two averaged molecules in the monoclinic unit-cell; space group  $P2_1/a$ ; see text). For  $0 \leq q/a^* < 0.5$  the figure shows symmetric modes with respect to the glide plane and for  $0.5 < q/a^* \leq 1.0$  antisymmetric ones.

rigid molecules in the unit cell six symmetrical and six antisymmetrical dispersion branches exist. The extended zone scheme is particularly useful in non-symmorphic space groups for directions in which the zone-boundary modes are doubly degenerate and merge smoothly into each other with opposite but finite slope as it is seen in  $[\xi, 0, 0]$  direction. Furthermore, at Y-point, the dispersion curves change the character of their representation. The extended zone scheme has the advantage that the dispersion branches must not cross. But modes of the same symmetry can exchange their eigenvectors at so-called anti-crossing points. During experiment two modes of the same eigenvector are connected at the zone boundary and can often be observed in going from one Brillouin-zone into a neighboring one.

At  $\Gamma$ -point one has four different representations.  $\Gamma_1$  and  $\Gamma_3$  contain symmetric and antisymmetric librations (plus possible contributions from internal  $g$ -type modes).  $\Gamma_2$  and  $\Gamma_4$  contain the external translations and eventual contributions from low internal  $u$ -type modes.

Provided model 1 describes the crystal correctly, the assignment of the representations  $\Gamma_1$  to  $\Gamma_4$  can be unambiguously obtained from measurements in the  $a^*-c^*$ -plane and along the  $b^*$ -axis. The  $\Gamma_2$  and  $\Gamma_3$  modes are invisible for Brillouin zones  $(h, 0, l)$  with  $h$  even as well as the dispersion curves in the  $[\xi, 0, 0]$  and  $[0, 0, \xi]$  directions, merging into  $\Gamma_2$  and  $\Gamma_3$ . For the  $\Gamma_1$  and  $\Gamma_4$  modes and the dispersion branches the extinction condition is just opposite, i.e. they are invisible for odd  $h$  in  $(h, 0, l)$ -zones. Along the  $b^*$ -axis  $\Gamma_1$  and  $\Gamma_2$  are invisible for odd  $k$  in  $(0, k, 0)$  zones and  $\Gamma_3$  and  $\Gamma_4$  are invisible for even  $k$ , respectively.

For light scattering experiments model 1 predicts that only the librational  $\Gamma_1$  and  $\Gamma_3$  modes are Raman active while the other ones can be found in an infrared absorption spectrum.

### 3.2. Model 2

Here, both A- and B-molecule in the monoclinic unit-cell are "up"-molecules (see Fig. 1b). B is related to A-molecule by the glide-reflection of the space group Pa, that means a reflection at the  $a$ - $c$ -plane through  $0.25 \mathbf{b}$  and a translation along  $\mathbf{a}/2$ .

In this model the same procedure for minimization of the lattice energy was performed as for model 1. But because the center of gravity of molecule A is not fixed to the origin of the unit cell by symmetry, the position of the center of gravity was also varied, in order to reach the minimum of the lattice energy.

Because the space group Pa contains identity and a glide plane,

the  $a^*-c^*$ -plane is the symmetry plane and there are two different representations in the  $[\xi, 0, \eta]$  direction. The dispersion curves in Figure 5 are given in the extended zone scheme. On the left side there are the symmetric modes with respect to reflection and on the other side there are the anti-symmetric ones. At the zone-boundary (Y-point) they degenerate because of time reversal symmetry. Calculations gave similar extinction conditions as we have mentioned: phonons which are symmetric with respect to the reflection at the  $a^*-c^*$ -plane can be seen in  $(h, 0, l)$ -zones with  $h$  even and the anti-symmetric ones in those, where  $h$  is odd. At the  $\Gamma$ -point there are

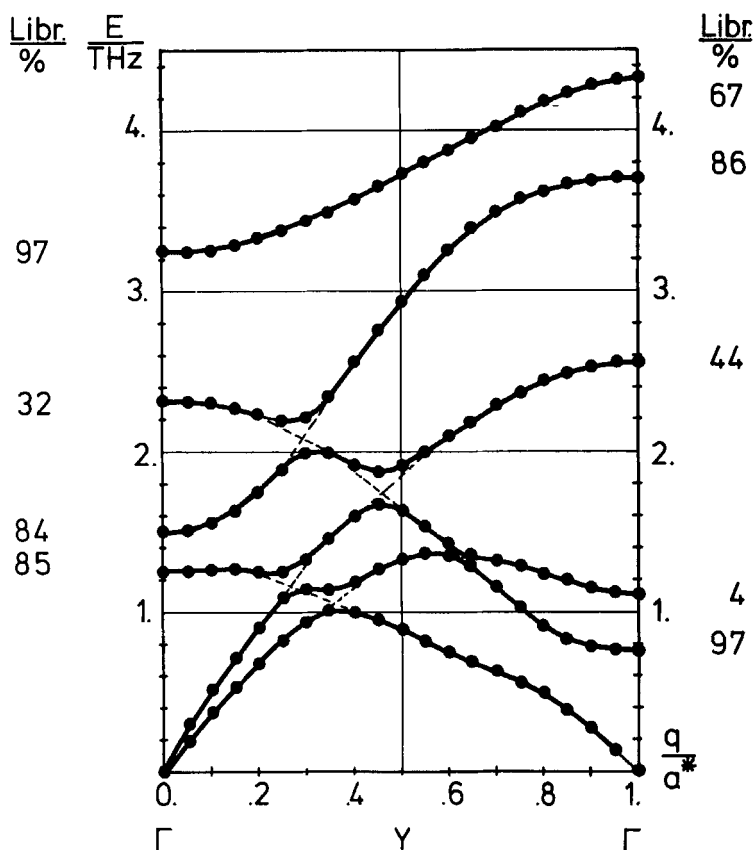


FIGURE 5 Calculated dispersion curves for 2,3-DMN in an extended zone scheme for the wavevector  $\mathbf{q}$  parallel to the  $[1, 0, 0]$ -direction using model 2 (see text). The figure shows for  $0 \leq q/a^* < 0.5$  symmetric modes with respect to the glide plane and for  $0.5 < q/a^* \leq 1.0$  the antisymmetric ones. The numbers on the left and right side of the diagram give the percentage of the librational energy of the  $\Gamma$ -modes.

TABLE III

The set of parameters (Williams IV set<sup>7</sup>) used for the model calculations.

	$A_n$ kJ mol <sup>-1</sup> nm <sup>-6</sup>	$B_n$ kJ mol <sup>-1</sup>	$\alpha_n$ nm <sup>-1</sup>
C-C	2.380 10 <sup>9</sup>	3.5041 10 <sup>6</sup>	36.0
C-D	5.238 10 <sup>8</sup>	3.6730 10 <sup>4</sup>	36.7
D-D	1.144 10 <sup>8</sup>	1.1120 10 <sup>4</sup>	37.4

still two irreducible representations of the point group. But here the librations or translations are not pure. Figure 5 shows for the  $\Gamma$ -modes the relative fraction of the librational energy.

### 3.3. Model 3

In this model the A-molecules are “up”-; the B-molecules are “down”-molecules (see Figure 1c). In the monoclinic unit-cell the B molecule is related to A by the screw diade operation of space group  $P2_1$ , that means a rotation around the crystallographic **b**-axis and a translation along  $(\mathbf{a} + \mathbf{b})/2$ .

The lattice energy was minimized as in model 2. Since the space group  $P2_1$  contains as symmetry elements the identity and a two-fold screw operation around the *b*-axis, the  $a^*-c^*$ -plane is not a plane of symmetry and all modes in this plane, except at the  $\Gamma$ -point and at the zone-boundary, belong to the same representation. All dispersion curves must be given in an usual zone scheme (see Figure 6) and are not allowed to cross. Degeneracies of phonon modes at the Y-point are accidental. At the  $\Gamma$ -point only two representations  $\bar{\Gamma}_1$  and  $\bar{\Gamma}_2$  exist and the librations or translations are not pure. In Figure 6 the left column gives the relative part of the librational energy at the  $\Gamma$ -point.

The calculated unit cell parameters for the different models, as well as the measured values are listed in Table IV. Especially for the parameters *a* and  $\beta$  a discrepancy exists between calculated and measured values.

We speculate that at least the order of magnitude of the width of the phonon dispersion curves is in some way related to the differences in phonon energies of these three simple models. Taking into account the character of the phonons (that means we look for nearly identical eigenvectors) of the phonons one can find nearly always a one-to-one correspondence between the phonon dispersion curves of the three models. The frequency differences for such equal phonons should give an estimate for the linewidth of the phonon and we expect to

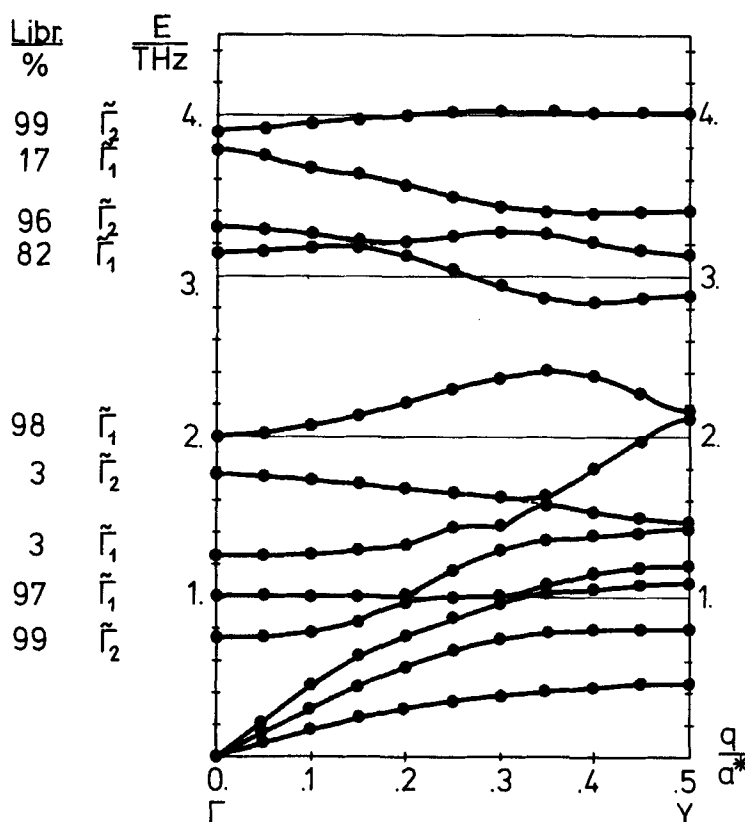


FIGURE 6 Calculated dispersion curves for 2,3-DMN for the wavevector  $q$  parallel to the  $[1,0,0]$ -direction in the usual zone scheme using model 3.  $\Gamma_1$  and  $\Gamma_2$  are the representations of the crystal's point group at the  $\Gamma$ -point (see text). The numbers on the left side give the percentage of the librational energy of the  $\Gamma$ -modes.

find for some of the phonons a width which can amount to nearly 1.0 THz. This indeed was found experimentally.

#### 4. DISCUSSION OF THE RESULTS

If one compares the results of calculations for the  $[1,0,0]$ -direction using models 1 and 2, one can see rough similarity with respect to the phonon frequencies and the polarization vectors of the modes through the whole Brillouin-zone. A comparison at the  $\Gamma$ -point with the results using model 3 gives a similar degree of similarity, but it becomes worse within the Brillouin-zone.



TABLE IV

The values of the experimental and calculated lattice parameters.

From experiment:			From calculation:		
lattice para- meter	x-ray data (ref. 1)	present neutron experiment	after minimization of lattice energy		
			model 1	model 2	model 3
	proto- nated 2,3-DMN	2,3-DMN	deuterated deuterated 2,3-DMN		
	300 K	123 K			
a/nm	0.7916(10)	0.768(1)	0.7167	0.7663	0.7484
b/nm	0.6052(8)	0.593(1)	0.6073	0.6225	0.6127
c/nm	1.0017(8)	0.988(2)	0.9933	0.9715	1.0694
$\beta/^\circ$	105.431(10)	104.47(3)	109.42	108.54	114.54
lattice energy in kJ mol <sup>-1</sup> :			-56.812	-56.544	-55.568

We study whether the extinction conditions for phonons calculated for the models 1 and 2 are approximately fulfilled in the experiment. The measured phonon intensities which according to models 1 and 2 are strictly forbidden are at least weak in comparison for the other ones and therefore we assigned the phonons found in Brillouin-zones ( $h,0,l$ ) with  $h$  even to the left side of the extended zone scheme and with  $h$  odd to the right side (see Table I and Figure 3). The validity of the extinction conditions found for the three models and in the experiments should still be tested in more detail in a further experiment with better statistics.

It is reasonable to use the results known from the Raman experiment (represented at the right side in Figure 3) and to compare these results with those obtained from the neutron experiment at the  $\Gamma$ -point (see Table II). Raman results give only  $\Gamma$ -modes with librational character, provided model 1 is valid. Within the framework of models 2 and 3 all  $\Gamma$ -modes are Raman active in principle, but it is expected that in reality modes which exhibit a predominant librational character have much more intensity than the other ones. Therefore all new  $\Gamma$ -modes not found by the Raman-experiment should have essentially translational character.

In the extended zone scheme the dispersion curves of the same symmetry must not cross. Near the anticrossing points an exchange of eigenvectors between the different branches occurs. This gives rise

to an exchange of the measured intensities of these branches and we could follow experimentally the intensities and halfwidths of the phonons.

If possible we followed modes even crossing zone-boundary, for example the longitudinally polarized acoustic mode on the symmetric side up to the Y-point, where it has an energy of 1.90(5) THz. This mode was seen again for  $0.7 \leq q/a^* \leq 1.0$  on the antisymmetric side (branch 5) with energies from 2.46(12) to 3.14(15) THz. The open circles in Figure 3 indicate weak intensities only, but these phonons are confirmed by a later experiment.

The acoustic phonons with transversal polarisation in *c*-direction, mentioned in section 2, are represented in branch 1 up to the zone-boundary. Modes with similar character are seen again on the anti-symmetric part of branch 3 (see Figure 3). The phonons there should have predominantly translational transversal character; the energy at the zone-center amounts to 0.99(5) THz.

The phonons of branch 1 on the antisymmetric side could not be detected during this experiment with the  $a^*-c^*$ -plane chosen as scattering plane. This is in agreement with the model calculations that predict these transversal acoustic phonons polarized in *b*-direction. The phonon intensities on the left (symmetric) part of branch 5 near  $\Gamma$ -point is very low. We believe that these phonons are essentially *b*-polarized, and that the visibility is due to some weak librational character. The calculations with models 2 and 3 show indeed that these modes have some librational character.

Branch 6 in Figure 3 should be the librational mode with highest energy. This mode was found in the  $[-2,0,1]$ -zone and we followed it across the zone-boundary into the  $[-3,0,1]$ -zone.

According to the calculation, the librations about molecular axes with increasing moment of inertia should have decreasing energies. In our opinion the horizontal parts of branches 2, 4 and 6 (see Figure 3) show *a*, *b* and *c* polarized librational characters.

It was not possible to follow branch 2 across the zone-boundary, because of a possible change of polarization to *b*-direction the intensity of the phonons was lost in the present experiment. Therefore, it is not clear to what branch the phonon  $q = 0.4a^*$ ,  $\nu = 0.83(3)$  THz (see Figure 3) belongs.

An attempt was made to compare calculated dynamical structure factors in different Brillouin-zones with the experimental data. Up to now a comparison gives no clear preference to any of the models used, because only part agreement was found in either case.

Figure 3 shows a few phonons, which could not be assigned to a definite branch until now:

$q/a^*$	0.0	0.1	0.5	1.0
$\nu/\text{THz}$	4.33(13)		4.41(7)	4.44(23)
	4.04(9)	4.02(3)	3.99(4)	4.18(12)

The phonons with frequencies of about 4.05 THz probably belong to an internal mode with small dispersion as it is assumed in Reference 3. In naphthalene and anthracene there are corresponding modes.

Four weak phonons observed at energies from 4.18 to 4.44 THz could be related with librations of the  $\text{CD}_3$ -group about the three-fold axis of symmetry. This mode is expected at 4.34 THz<sup>4</sup> as mentioned before in the Introduction.

## 5. CONCLUSION

Coherent inelastic neutron scattering on 2,3-DMN crystals led to a determination of dispersion curves along the  $[1,0,0]$ -direction. Using results from a Raman experiment and with the help of calculations, it was possible to determine the predominant motional character of the different modes at the  $\Gamma$ -point and within the Brillouin-zone. For these calculations a rigid body model for the molecules in crystals of different space groups was used. Up to frequencies of about 3.9 THz the lattice dynamics of 2,3-DMN display features which are similar to the lattice dynamics of pure naphthalene. One striking difference, however, is a broadening of the phonons in 2,3-DMN caused by dipolar disorder, which amounts to up to 1.0 THz. The order of magnitude of the width can qualitatively be explained by the results of model calculations for some artificially constructed translational invariant ideal crystals. Phonons found with energies above 3.9 THz were ascribed to be internal ones. An internal mode is expected for a frequency of  $\approx 4$  THz and a librational mode of the  $\text{CD}_3$ -groups for  $\approx 4.3$  THz.

## Acknowledgments

This work has been funded by the German Federal Minister for Research and Technology (BMFT) under contract number 03-KA1BAY-0. We thank the Kernforschungs-

anlage Jülich for support; discussions with Dr. Natkaniec are gratefully acknowledged. We thank Prof. N. Karl from the Technische Universität Stuttgart for discussions and preparation of the single crystals.

## References

1. N. Karl, H. Heym and J. J. Stezowski, *Mol. Cryst. Liq. Cryst.*, **131**, 163 (1985).
2. N. Karl, *Mater. Sci. (Wroclaw)*, **10**, 365 (1984).
3. J. Kalus, H. Gerlach, J. Schleifer, F. Wörlen, G. Voß, M. Godlewska, I. Natkaniec, N. Karl and M. Prager, *Phys. Stat. Sol. (b)*, **134**, 53 (1986).
4. J. Kalus, J. Schleifer, R. Hempelmann and W. Richter, *Phys. Stat. Sol. (b)*, **136**, 513 (1986).
5. D. Weaire, P. C. Tylor, W. M. Visscher and J. E. Gubermatis, *Dynamical Properties of Solids, Vol. 4*; R. J. Elliott and P. L. Leath, *Dynamical Properties of Solids, Vol. 2*, eds., G. H. Horton and A. A. Maradudin, (North-Holland Publ. Co., Amsterdam/New York/Oxford, 1980).
6. G. S. Pawley, *Phys. Stat. Sol. (b)*, **49**, 475 (1972).
7. D. E. Williams, *J. Chem. Phys.*, **47**, 4680 (1967).
8. B. Dorner, E. L. Bokhenkov, S. L. Chaplot, J. Kalus, I. Natkaniec, U. Schmelzer and E. F. Sheka, *J. Phys. C: Sol. State Phys.*, **15**, 2353 (1982).